Published in final edited form as:
*Cell*. 2014 July 3; 158(1): 69–83. doi:10.1016/j.cell.2014.04.049.

# IRF4 is a key thermogenic transcriptional partner of PGC-1α

**Xingxing Kong**[1], **Alexander Banks**[2,#], **Tiemin Liu**[1,^], **Lawrence Kazak**[2], **Rajesh R. Rao**[2], **Paul Cohen**[2], **Xun Wang**[1], **Songtao Yu**[3], **James C. Lo**[2], **Yu-Hua Tseng**[4], **Aaron M. Cypess**[4], **Ruidan Xue**[4], **Sandra Kleiner**[2,†], **Sona Kang**[1], **Bruce M. Spiegelman**[2], and **Evan D. Rosen**[1,5,*]

[1]Division of Endocrinology, Beth Israel Deaconess Medical Center and Department of Genetics, Harvard Medical School, Boston, MA 02215, USA

[2]Dana-Farber Cancer Institute and Department of Cell Biology, Harvard Medical School, Boston, MA 02215, USA

[3]Department of Pediatrics, Children's Memorial Research Center, Northwestern University Feinberg School of Medicine, Chicago, IL 60614, USA

[4]Section on Integrative Physiology and Metabolism, Joslin Diabetes Center, Harvard Medical School, Boston, Massachusetts 02215, USA

[5]Broad Institute, Cambridge, MA 02142, USA

## Summary

Brown fat can reduce obesity through the dissipation of calories as heat. Control of thermogenic gene expression occurs via the induction of various co-activators, most notably PGC-1α. In contrast, the transcription factor partner(s) of these co-factors are poorly described. Here we identify interferon regulatory factor 4 (IRF4) as a dominant transcriptional effector of thermogenesis. IRF4 is induced by cold and cAMP in adipocytes and is sufficient to promote increased thermogenic gene expression, energy expenditure, and cold tolerance. Conversely, knockout of IRF4 in $UCP1^{+}$ cells causes reduced thermogenic gene expression and energy expenditure, obesity, and cold intolerance. IRF4 also induces the expression of PGC-1α and PRDM16, and interacts with PGC-1α, driving *Ucp1* expression. Finally, cold, β-agonists, or forced expression of PGC-1α are unable to cause thermogenic gene expression in the absence of



*Corresponding author Direct correspondence to erosen@bidmc.harvard.edu.
#Current affiliation: Division of Endocrinology, Brigham and Women's Hospital, Boston, MA 02215, USA
^Current affiliation: Division of Hypothalamic Research, University of Texas Southwestern Medical Center, Dallas, TX 75235, USA
†Current affiliation: Genomics Institute of the Novartis Research Foundation, San Diego, CA 92121, USA



**Author Contributions**

X.K. designed and performed all experiments, analyzed the data, and edited the manuscript. A.B., J.C.L. and S.K. analyzed energy expenditure and edited the manuscript. T.L. designed and performed animal experiments, analyzed the data, and edited the manuscript. L.K. performed the Seahorse experiments. R.R.R. performed the adenovirus injection into the inguinal fat depots. S.Y. designed and developed the *UCP1-Cre* mouse. Y.T., A.M.C. and R.X. performed the human primary adipocyte experiments. P.C., X.W. and S.K. assisted with various additional experiments. B.M.S. designed experiments and edited the manuscript. E.D.R. devised and supervised the experimental plan and wrote the manuscript.

IRF4. These studies establish IRF4 as a transcriptional driver of a program of thermogenic gene expression and energy expenditure.

## Introduction

Although many creatures can produce heat, only eutherian mammals possess brown adipocytes, specialized cells that use uncoupling protein 1 (UCP1) to dissociate $O_2$ consumption from ATP synthesis. This highly thermogenic process consumes large amounts of substrate (primarily fatty acids, but also glucose), and is activated by cold exposure, catecholamines, and other stimuli (Villarroya and Vidal-Puig, 2013). Two different $UCP1^+$ cell types have been described, so-called 'classic' brown adipocytes, which are present at all times in the interscapular region of rodents, and a 'recruitable' cell called the beige adipocyte that develops within specific white adipose depots when environmental conditions demand it (Wu et al., 2013). These two $UCP1^+$ cell types derive from different embryological origins, and they express overlapping but distinct gene expression programs (Seale et al., 2008; Wu et al., 2012). The study of human brown fat has undergone a dramatic renaissance with the recent discovery that adults possess significant quantities of this tissue (Cypess et al., 2009; van Marken Lichtenbelt et al., 2009; Virtanen et al., 2009), opening the door for therapeutic manipulation of these cells in diabetes and obesity.

At the transcriptional level, most attention has fallen on various co-factors, which lack DNA binding domains and thus must act by docking on *bona fide* transcription factors. Among the best studied of these are PGC-1α and Prdm16, the latter of which acts through the transcription factors C/EBPp, PPARy, and possibly others to promote brown and beige adipocyte identity (Kajimura et al., 2009; Kajimura et al., 2008; Seale et al., 2007). PGC-1α has been shown to co-activate PPARy and PPARα to promote brown fat differentiation and fatty acid oxidation respectively; it drives mitochondrial biogenesis, at least in part, via its actions on ERRa (Wu and Boss, 2007). It is less clear, however, how the thermogenic gene expression program is co-activated by PGC-1α. For example, mice lacking ERRa have defects in mitochondrial number and function but still induce *Ucp1* expression appropriately when exposed to cold (Villena et al., 2007). Similarly, PPARα null mice display defective fatty acid oxidation, but normal thermogenic gene expression, including *Ucp1* (Xue et al., 2005).

We have previously identified interferon regulatory factor 4 (IRF4) as an important regulator of adipogenesis and adipose lipid handling (Eguchi et al., 2011; Eguchi et al., 2008). IRF4 expression is induced by fasting in adipocytes via FoxO1, and is repressed by insulin. Animals that lack IRF4 in adipose tissue are obese and insulin resistant, and are unable to fully mobilize lipid stores in the face of catecholamine treatment or prolonged fasting (Eguchi et al., 2011). Of note, these mice are also cold intolerant, a phenotype ascribed at the time to reduced fatty acid substrate required to fuel thermogenesis. Interestingly, however, we also noted that some thermogenic gene expression, including *Ucp1*, was reduced in the interscapular brown adipose tissue (BAT) of these animals. This led to the suggestion that, in addition to serving as a key regulator of lipolysis in both brown and white adipose tissues, IRF4 might also play a *direct* thermogenic role in the latter.

Here we show that IRF4 is transcriptionally regulated by cold and cAMP in murine and human BAT prior to the induction of *Ucp1*, and that mice that overexpress IRF4 transgenically in BAT display enhanced thermogenic gene expression, energy expenditure, and cold tolerance. Conversely, mice lacking IRF4 specifically in UCP1$^+$ cells are obese and insulin resistant, and display reduced thermogenic gene expression, cold tolerance, and energy expenditure. Importantly, IRF4 induces the expression of both *Ppargc1a* and *Prdm16*, and physically interacts with PGC-1α to induce *Ucp1* expression. Finally, cold, catecholamines, and forced expression of PGC-1α are unable to induce thermogenic gene expression in the absence of IRF4. Taken together, these studies demonstrate that IRF4 acts as a dominant transcriptional regulator of thermogenesis via genetic and physical interactions with PGC-1α.

## Results

### Irf4 expression is induced in brown adipocytes by cold and cAMP

Fasting induces *Irf4* in both WAT and BAT (Eguchi et al., 2011), and we wondered if cold exposure might have a similar effect. This proved to be the case, as 6 hours at 4°C increased both mRNA and protein levels of IRF4 in classical interscapular brown fat as well as in inguinal and epididymal white fat (Fig. 1A,B). Time course analysis shows that this effect occurs within an hour of cold exposure, coincident with the induction of *Ppargc1a* and prior to *Ucp1* (Fig. 1C). *Irf4* mRNA was also induced after the administration of the β3-agonist CL-316,243 (Fig. 1D). To test whether these effects are cell autonomous, we harvested the stromal-vascular fraction (SVF) from the brown fat pads of newborn mice and differentiated them *ex vivo;* treatment of these cells with forskolin caused a significant elevation in *Irf4* mRNA levels (Fig. 1E). Recently, cultured 3T3-F442A adipocytes were shown to induce a thermogenic gene expression program when exposed directly to 30°C (Ye et al., 2013). We tested whether *Irf4* expression is also sensitive to this perturbation and found a modest but significant induction by cold even in these isolated cells (Fig. 1F), suggesting the involvement of cell autonomous mechanisms that do not require catecholamine signaling.

UCP1$^+$ adipocytes have now been unequivocally identified in adult humans (Cypess et al., 2009; van Marken Lichtenbelt et al., 2009; Virtanen et al., 2009). There is still ambiguity over whether these cells correspond to murine brown or beige fat, with one study suggesting that more superficial neck deposits are similar to beige while deeper depots correspond to classic brown fat (Cypess et al., 2013). We found that cAMP treatment dramatically induced *Irf4* mRNA expression in adipocytes derived from both deep and superficial human depots (Fig. 1G).

### Targeted expression of IRF4 causes enhanced energy expenditure and leanness

Having established that IRF4 expression is elevated in the BAT and WAT of cold-exposed animals, we asked whether IRF4 is sufficient to promote thermogenesis. To this end, we developed a new line of knock-in mice in which the IRF4 cDNA was inserted downstream of the ROSA26 promoter and a loxP-Stop-loxP cassette (R26-LSL-IRF4; Fig. S1A). Crossing these mice to Ucp1-Cre mice would then enable targeted overexpression in brown adipocytes. Unfortunately, the available Ucp1-promoter driven Cre line (Guerra et al., 2001)

has problems with both specificity and recombination efficiency. We thus generated a new Ucp1-Cre line using a BAC transgenic approach. By inserting the Cre recombinase cassette into the starting ATG of *Ucp1* within a large bacterial artificial chromosome (Fig. S1B), we ensured that the majority of the key regulatory elements would be in their native context. At room temperature, these mice express Cre specifically in the interscapular brown fat (Fig. S1C). Cold exposure induces Cre expression in inguinal and epididymal WAT in a time-dependent manner, consistent with the onset of browning (Fig. S1D). Importantly, these mice do not have any obvious metabolic phenotype (Fig S1E,F; Fig S2A).

Mice that carry both the Ucp1-Cre and R26-LSL-IRF4 transgenes (hereafter designated as BAT IRF4 overexpressors, or BATI4OE) exhibit moderate (5–10X) overexpression of IRF4 in BAT (Fig. 2A,B), in the range of the induction seen following exposure to cold or β-agonist. No overexpression is seen in inguinal or epididymal depots at room temperature. BATI4OE mice display significantly reduced body weight and fat mass on both chow (Fig. S2A,B) and high fat diets (Fig. 2C,D). Both inguinal and epididymal depots are smaller in BATI4OE mice, and their adipocytes show less hypertrophy on a high fat diet than those of control mice (Fig. 2E,F, S2C). Food intake did not differ between the genotypes (Fig. 2G), but BATI4OE mice had enhanced energy expenditure (Fig. 2H,I); physical activity was unchanged (Fig. S2D). In addition, we assessed the effect of IRF4 overexpression in BAT on glucose homeostasis and found that overexpressor mice have improved glucose and insulin tolerance testing relative to controls on a high fat diet (Fig. S2E,F).

## IRF4 expression is sufficient to cause enhanced thermogenesis in BAT

BATI4OE mice have smaller brown adipose depots (Fig. S2C,Fig. 3A) and reduced lipid stores in BAT at both room temperature and 4°C (Fig. 3B). This phenotypic change is accompanied by increased expression of key thermogenic genes (e.g. *Ucp1*, *Prdm16*, and *Ppargc1a)* (Fig. 3C,D). Fatty acid oxidation genes (e.g. *Ppara*, *Cpt1b*) were also induced, consistent with a trend towards increased palmitate oxidation in BATI4OE brown adipocytes tested *ex vivo* (Fig. S2G). No change was seen in the expression of genes encoding mitochondrial proteins (Fig. 3C), although some changes are seen in the mitochondrial protein levels themselves (Fig. S2H). Isolated mitochondria from the BAT of BATI4OE mice display increased uncoupled respiration (Fig.3E). General adipose markers are unaffected in these mice, as were lipolysis genes (Fig. 3F), consistent with unaltered lipolysis in brown adipocytes *ex vivo* and BATI4OE mice *in vivo* (Fig. S2I,J). Interestingly, lipogenesis was significantly reduced in brown adipocytes from BATI4OE mice (Fig. S2K), although genes like *Fasn*, *Srebf*, and *Scd1* are unaltered (Fig. 3F). Consistent with the changes in thermogenic gene expression, BATI4OE mice are modestly but significantly better able to defend their body temperature during an acute cold stress (Fig. 3G).

We also assessed whether overexpression of IRF4 could affect the browning of white adipose depots. As expected, BATI4OE mice do not show elevated IRF4 levels in inguinal WAT at room temperature, as there is minimal *Ucp1* expression in that condition, and thus no recombination. Exposure to cold for 6 days increased *Irf4* expression in both control and BATI4OE mice such that the final levels were equivalent in the two lines. Consistent with this, we saw no difference in thermogenic gene expression or in the histological appearance

of inguinal fat (Fig. S3A,B). In epididymal fat, however, we did see increased *Irf4* expression in BATI4OE mice, accompanied by increased thermogenic gene expression and a histological pattern consistent with enhanced browning (Fig. S3C,D).

## Loss of IRF4 in brown fat causes reduced energy expenditure and predisposes to obesity

It is well established that obese animals and humans show deficiencies in BAT content and function (Ricquier et al., 1986; Saito et al., 2009; Tokuyama and Himms-Hagen, 1986; van Marken Lichtenbelt et al., 2009; Vijgen et al., 2011; Virtanen et al., 2009), and consistent with this, we see reduced *Irf4* expression in the interscapular BAT of high-fat fed mice as well as in two genetic models of obesity (*ob/ob* and *db/db*) (Fig. 4A).

Of course this association does not prove causality, so we generated animals lacking IRF4 specifically in BAT by crossing our Ucp1-Cre line to $Irf4^{flox/flox}$ mice (Klein et al., 2006). The resulting $Irf4^{flox/flox};Cre^{+}$ animals (henceforth designated as BAT IRF4 knockout, or BATI4KO) have remarkably little IRF4 mRNA or protein left in the interscapular BAT at room temperature (Fig. 4B,C), while other tissues, such as WAT and spleen, show no change. Resident macrophages and T cells, which express high levels of IRF4 but do not express *Ucp1*, likely account for the small amount of residual IRF4 seen in BAT. On chow diet, male BATI4KO mice display a tendency toward higher body weight (Fig. S4A), and have a small but significant increase in fat mass (Fig. S4B). On a high fat diet, the BATI4KO mice clearly have elevated body weight and adiposity (Fig. 4D,E). The white adipose depots of BATI4KO mice are hypertrophic relative to $Irf4^{flox/flox};Cre^{™}$ littermates (Fig. 4F,G, S4C). The cause of the increased adiposity seen in BATI4KO mice was not increased food intake, as this did not differ between these mice and their controls (Fig. 4H). Rather, large reductions were seen in both oxygen consumption and $CO_2$ production (Fig. 4I,J) without altered physical activity (Fig. S4D).

As would be predicted from their elevated body weight, BATI4KO mice show worsened glucose and insulin tolerance (Fig. S4E,F). To determine whether this could be fully ascribed to obesity, we repeated the glucose and insulin tolerance tests on mice exposed to a high-fat diet for only 4 weeks, a time point prior to the divergence in body weight. These mice still showed significant glucose and insulin intolerance under these conditions (Fig. S4G,H), indicating that increased body weight is not the primary driver of the metabolic defect. Although some BATI4KO mice appeared to be longer than their control littermates, this was not significant between the groups as a whole (N=8–11).

## IRF4 is required for normal thermogenesis and mitochondrial function in BAT

Reduced energy expenditure, obesity, and dysglycemia are all hallmarks of deficient brown adipose function, and suggest a defect in thermogenic capacity. The interscapular brown adipose depot from BATI4KO mice was grossly larger and showed hypertrophic cells with increased lipid content at room temperature (Fig. 5A,B, Fig. S4C). At 4°C, both genotypes showed reduced lipid in BAT, although a significant difference was still noted (Fig. 5B). This was accompanied by a clear reduction in the expression of genes associated with thermogenesis, electron transport, and fatty acid oxidation (Fig. 5C,D). As predicted by the gene expression changes, palmitate oxidation in BATI4KO cells was significantly reduced

(Fig. S5A). In accordance with our prior work (Eguchi et al., 2011), we saw significant reductions in lipolytic gene expression, accompanied by diminished lipolytic activity *ex vivo* and *in vivo* (Fig. S5B,C). As was seen in the overexpressor mice, lipogenic activity was altered even though lipogenic gene expression was not (Fig. 5E, S5D).

BATI4KO mice show reduced mitochondrial respiration (Fig. 5F,G) and gene expression (Fig. 5C, S5E). At the ultrastructural level, however, the mitochondria of BATI4KO mice appear indistinguishable from their controls, both in terms of overall number and in the density of cristae (Fig. S5F,G,H). We next exposed BATI4KO and control mice to 4°C and measured body temperature, to assess the physiological importance of these defects. As predicted, BATI4KO mice were less able to defend their body temperature in the face of acute cold stress (Fig. 5H).

We also wished to assess the requirement for IRF4 in the browning of white fat. We were concerned that our system is not optimized to answer this question, because Cre-mediated recombination will not occur until after cold drives the differentiation of these cells (Wang et al., 2013). Despite this caveat, however, BATI4KO mice exposed to 4°C for 6 days display reduced thermogenic and mitochondrial gene expression in their inguinal WAT relative to control mice (Fig S6A). This was consistent with the cold-dependent appearance of small, multilocular $UCP1^+$ cells in control, but not BATI4KO mice (Fig. S6B). No change was seen in the histological appearance or gene expression pattern of epididymal fat in these mice (Fig. S6C,D).

## Thermogenic gene expression cannot be induced by cold or β-agonists in the absence of IRF4

Having determined that IRF4 is required for basal thermogenic gene expression in brown and beige adipocytes, we next asked whether this program could still be provoked in the absence of IRF4. We first assessed this in cold-exposed animals, showing that many thermogenic genes such as *Ucp1, Dio2*, and *Ppargc1a* become induced in the interscapular BAT of floxed control mice, but not BATI4KO mice (Fig. 6A). Similarly, the CL-316,243 induces a broad array of genes that promote thermogenesis, fatty acid oxidation, and lipolysis in control mice, while BATI4KO mice do not recapitulate this effect (Fig. 6B).

## PGC-1α and IRF4 interact genetically, physically, and functionally

IRF4 is induced in BAT contemporaneously with PGC-1α (Fig. 1C), and is required for the full expression of PGC-1α in both the basal and stimulated states (Fig. 5C, Fig. 6A, Fig. 6B). We next asked whether the converse is also true; is PGC-1α required for *Irf4* expression? We first looked at the BAT of mice lacking *Ppargc1a* in adipose tissue (Kleiner et al., 2012), and saw that, in fact, *Irf4* mRNA levels were approximately 1/3 of those seen in wild-type control animals (Fig. S7A). Furthermore, we took SVF cells from the inguinal fat of these mice and differentiated them *ex vivo;* treatment with forskolin caused a significant induction of *Irf4* mRNA in wild-type cells that was severely blunted in cells lacking PGC-1α (Fig. S7B). Together, these data suggest that PGC-1α and IRF4 induce each other's expression in a mutually reinforcing loop.

We also asked whether IRF4 and PGC-1α interact physically. The phenomenon in which a transcription factor induces the expression of a co-activator and then interacts with that factor to regulate downstream gene expression is considered a form of feed-forward regulation (Alon, 2007; Wu et al., 1999). In a co-immunoprecipitation assay *in vitro*, we found that PGC-1α interacts strongly with IRF4 (Fig. 7A). This could be recapitulated in isolated brown adipocytes from cold-exposed mice, demonstrating that the interaction occurs at normal levels of these two proteins (Fig. 7B). Furthermore, the interaction is direct, as it occurs even in a GST pull-down assay *in vitro* (Fig. 7C). Nuclear receptors, like PPARγ and ERRα, interact with PGC-1α via LXXLL motifs found in the N-terminal half of the molecule (Huss et al., 2002; Schreiber et al., 2003). We used various truncation mutants of PGC-1α to show that IRF4 docks on the same part of the molecule (Fig. S7C,D). Specifically, deletion of the second and third LXXLL motifs of PGC-1α completely blocks the interaction with IRF4 (Fig. S7E). IRF4, like other members of the IRF family, has a large C-terminal region used for protein-protein interactions (IAD), such as with PU.1 or other IRFs (Fig. S7F)(Honda and Taniguchi, 2006). Deletion of the IRF4 DBD does not disrupt the interaction with PGC-1α, but removal of the IAD does (Fig. S7G).

We also examined the 5' flanking region of the *Ucp1* gene to determine whether IRF4 might serve as a direct transcriptional regulator. Computational analysis identified a consensus interferon-stimulated response element (ISRE) located 1251 base pairs upstream of the transcriptional start site. A *Ucp1* promoter-luciferase construct transfected into 293 cells could be activated independently by IRF4 and by PGC-1α, and the two together caused an additive induction (Fig. 7D). A smaller construct (-1727) that still contains the ISRE showed even more impressive activation by PGC-1α and IRF4, suggesting distal negative regulatory elements. However, deletion of the ISRE abolished the induction of luciferase expression by IRF4, PGC-1α, or both. Similar results were obtained when primary BAT cells were used (Fig. S7H). IRF4 binds to this site on the *Ucp1* promoter in BAT, as shown by chromatin immunoprecipitation (Fig. 7E).

Finally, we forced overexpression of PGC-1α directly in the inguinal white fat of mice using adenoviral delivery. Even the modest level of overexpression achieved (≈50% increase over basal) was sufficient to induce thermogenic gene expression in this depot in wild-type mice. BATI4KO mice, however, did not show this effect, demonstrating definitively that PGC-1α is not thermogenic in the absence of IRF4 (Fig. 7F). Our data thus strongly suggest a model in which PGC-1α and IRF4 induce each others' expression and then interact physically to fully activate *Ucp1* (Fig. 7G).

## Discussion

Adaptive (non-shivering) thermogenesis relies upon the successful execution of a defined program of gene expression in response to ambient conditions, centered on *Ucp1*. In general, transcription requires the concerted actions of sequence-specific DNA binding proteins as well as a large number of co-factors, which do not themselves bind to DNA. These co-factors can activate or repress transcription, depending upon their ability to recruit specific chromatin-modifying enzymes to the locus being regulated. Interestingly, while a few sequence-specific transcription factors that play a role in brown fat differentiation and

function have been identified, such as PPARα, PPARγ, C/EBPp, EBF2, and ERRα, a much larger number of co-factors have been described (Kajimura et al., 2010; Rajakumari et al., 2013). These include pocket proteins like pRb and p107, but also SRC-1, SRC-2, SRC-3, TRIP-Br2, RIP140, and most notably, PRDM16 and PGC-1α (Kajimura et al., 2010; Liew et al., 2013; Puigserver and Spiegelman, 2003). The challenge, then, has been to identify the transcriptional partners through which these co-factors act to promote their activities.

Most of the published data on transcription and brown fat relate to the processes of development and the establishment of brown fat identity. Our work focuses instead on the transcriptional basis for thermogenic function in already differentiated brown and beige adipocytes. Specifically, the use of Ucp1-Cre mice to target ablation or overexpression of IRF4 requires that brown fat identity be *already established*. We have previously shown that IRF4 is moderately antiadipogenic (Eguchi et al., 2008); the actions we have focused on here and in our prior work in which we knocked out *Irf4* using an adiponectin-Cre deletor strain (Eguchi et al., 2011) are studies of adipocyte physiology, not specification or differentiation.

Brown and beige adipocytes are defined in part by their rich complement of mitochondria. PGC-1α is a major driver of mitochondrial biogenesis and function, subserving this function through interactions with ERRα and NRF-2 (Giguere, 2008). IRF4 does not promote mitochondrial gene expression when overexpressed in brown adipocytes, although we do see significantly reduced gene expression when IRF4 is ablated, associated with reduced oxygen consumption. Even in this condition, however, there is no change in mitochondrial number or appearance. This suggests that the interaction of PGC-1α and IRF4 to promote thermogenesis is distinct from an effect on mitochondrial biogenesis. In contrast, IRF4 is both necessary and sufficient to promote the fatty acid oxidation gene program, including expression of the dominant transcription factor of that process, PPARα.

We previously showed that loss of IRF4 in all fat (using the adiponectin-Cre line) diminishes isoproterenol-stimulated glycerol release by 30–50% (Eguchi et al., 2011), an effect seen both *ex vivo* and *in vivo*. Somewhat surprisingly, in the present work, loss of IRF4 restricted to $Ucp1^{+}$ cells has a quantitatively similar effect on lipolysis (Fig. S5B,C). Taken at face value, this suggests that BAT is the dominant source of liberated glycerol after a catecholamine challenge, despite the fact that BAT represents a small percentage of total fat mass. In fact, this may be a reasonable expectation, given that the β-adrenergic receptors *Adrb1*, *Adrb2*, and *Adrb3* are all expressed to a greater degree in BAT than in WAT (biogps.org); isoproterenol is a non-selective agonist of all three subtypes. Thus, BAT may be poised to transduce the catecholaminergic signal much more rapidly than WAT, and elevated glycerol levels in the first few hours after adrenergic stimulation may derive almost entirely from brown adipocytes. Perhaps depletion of BAT lipid stores might occur with longer periods of fasting, cold, or adrenergic agonist administration, allowing WAT to become the dominant source of lipolytic products. Testing this hypothesis will require careful tracer studies to identify the source of serum glycerol after a lipolytic provocation.

Our previous work also demonstrated that IRF4 was anti-lipogenic in white fat, such that loss of IRF4 in white adipocytes increased expression of such key lipid synthesis genes as

*Scd1*, *Fasn*, and *Srebf1*. Concordant with this, loss of IRF4 enhanced $^{14}$C-glucose incorporation into lipid, and add-back of IRF4 repressed this (Eguchi et al., 2011). In the current study, we find that loss of IRF4 in brown fat also increases lipid synthesis from glucose, and overexpression inhibits it. However, we see no concomitant change in lipogenic expression in either the gain-of-function or loss-of-function models to explain this. Possibly there are differences in levels of lipogenic enzyme protein or activity, or perhaps IRF4 is exerting its primary effects at the level of lipolysis and fatty acid oxidation, and the changes in lipid synthesis simply reflect altered substrate availability.

IRF4, unlike many other IRFs, is regulated strongly at the transcriptional level. In our previous work, we demonstrated that expression of *Irf4* mRNA is induced by fasting in both brown and white adipocytes (Eguchi et al., 2011). This effect is due to the drop in insulin levels that occurs in the fasted state, allowing FoxO1 to remain in the nucleus where it drives the *Irf4* promoter. Interestingly, Serrano's group recently showed that mice overexpressing *Pten* have enhanced FoxO1 activity and are lean with increased *Ucp1* and *Ppargc1a* expression (Ortega-Molina et al., 2012). Could FoxO1 be activated by cold, and thus serve as the upstream effector of IRF4 expression in BAT? A recent report demonstrates that FoxO1 is induced by 24 hours of cold exposure in rat muscle, with a subsequent increase in proteolysis (Manfredi et al., 2013). Thus, FoxO1 is an excellent candidate for a cold-inducible activator of IRF4 and subsequent thermogenesis. Other factors may also be at play, such as CREB, which mediates many of the transcriptional effects of cAMP (Altarejos and Montminy, 2011). Interestingly, a recent paper suggests that IRF4 acts *upstream* of CREB, at least in cardiac muscle (Jiang et al., 2013).

IRF4 plays a wide variety of roles in the immune system, including critical functions in macrophage polarization (Eguchi et al., 2013; Satoh et al., 2010), plasma cell differentiation (Klein et al., 2006; Sciammas et al., 2006), regulatory T cell function (Cretney et al., 2011; Zheng et al., 2009), and the differentiation of $CD4^+$ and $CD8^+$ T cells (Brustle et al., 2007; Kwon et al., 2009; Man et al., 2013; Raczkowski et al., 2013; Staudt et al., 2010; Yao et al., 2013). By and large, these studies have focused on a limited subset of IRF4 target genes that control immune cell differentiation, without considering a possible role for IRF4 as a regulator of energy metabolism, despite a longstanding appreciation of the enormous energy requirements inherent in mounting a coherent immune response (Odegaard and Chawla, 2013). One recent paper, however, did report that energy metabolism genes were direct targets of IRF4 in cytotoxic $CD8^+$ T cells, and even suggested that IRF4 ablation in these cells resulted in a reduced oxygen consumption rate (Man et al., 2013), consistent with what we find in brown adipose tissue. There has not been significant investigation into the role of PGC-1α in lymphocyte biology, although it is expressed in these cells (biogps.org), and one study does suggest a possible role for PGC-1α in regulating intralymphocyte antioxidant levels after exercise (Ferrer et al., 2009). In macrophages, the related co-activator PGC-1p is induced by Th2 cytokines like IL-4, promoting oxidative metabolism and reduced inflammatory gene expression. It is unknown if IRF4 interacts with PGC-1p, although this isoform does possess similar LXXLL domains as PGC-1α and is able to co-activate nuclear receptors (Meirhaeghe et al., 2003). Our results demonstrate that IRF4, alone or in

combination with PGC-1α, is a transcriptional regulator of cellular metabolism and support deeper investigation of this as a possible mechanism by which it acts in immune cells.

Transcriptional regulation of the *Ucp1* gene has been studied extensively. Early studies by the Kozak and Ricquier labs focused on a ∼200 bp region located approximately 2.5 kb upstream of the Ucp1 transcriptional start site. This area, originally defined by DNase I hypersensitivity, contains binding sites for transcription factors that mediate brown fat specification (PPARγ, EBF2) as well as cold and norepinephrine-induced thermogenesis (e.g. TR, CREB) (Boyer and Kozak, 1991; Kozak et al., 1994; Larose et al., 1996; Rajakumari et al., 2013). Here we isolate an interferon-stimulated response element (ISRE) mediating at least part of the IRF4 response that is separate from this narrowly defined enhancer. This region falls outside of all previously identified 5' flanking DNase hypersensitivity regions (Boyer and Kozak, 1991), but it should be noted that more recent studies from the mouse ENCODE consortium indicate that the entire 10 kb region proximal to the *Ucp1* TSS is heavily decorated by H3K4me1, H3K4me3, and H3K27ac marks in brown adipose tissue (https://genome.ucsc.edu/ENCODE/dataSummaryMouse.html). This indicates that a much larger region of this locus is characterized by open chromatin than has previously been appreciated.

Finally, it is worth remembering that non-shivering thermogenesis requires the coordinated activities of several different tissues. Cold must be sensed and signals sent via the sympathetic nervous system to release catecholamines, which activate β-adrenergic receptors in brown fat. Lipolysis in white fat must also occur to generate the fatty acid substrate required to fuel mitochondrial activity. Alternatively activated (so-called M2) macrophages have recently been proposed to participate in thermogenesis via their own elaboration of catecholamines (Nguyen et al., 2011). IRF4 has now been shown to be a key regulator of all of these processes: it is required for lipolysis in white fat (Eguchi et al., 2011) and for M2 polarization of macrophages (Eguchi et al., 2013; Satoh et al., 2010), and we now show that there is a direct effect of IRF4 on thermogenic gene expression in BAT. Taken together, these data establish IRF4 as a central actor in adaptive thermogenesis, acting to coordinate the activities of multiple tissues to generate heat.

## Experimental Procedures

### Antibodies

Antibodies were purchased from Santa Cruz Biotechnology (IRF4, sc-6059; actin, sc-1615; PGC-1α, sc-13067), Abcam (UCP1, AB10983; Mito profile, AB110413; Aconitase, AB110321), and Millipore (PGC-1α, ST1202-1SET).

### Animals

Mice were maintained under a 12hr light/12hr dark cycle at constant temperature (23°C) with free access to food and water. All animal studies were approved by the Institutional Animal Care and Use Committee of Beth Israel Deaconess Medical Center. For determination of IRF4 expression in fat depots from mice exposed to cold, mice were housed at 4°C for up to 6 days. The 16-week-old *ob/ob* and *db/db* mice were purchased from

Jackson Laboratories. For DIO studies, C57BL/6J mice were fed a high-fat diet (D12331; Research Diets) for 12 weeks.

### Cold-Induced Thermogenesis

Mice were placed in a cold chamber (4°C) for up to one week. Body temperature was measured using a rectal probe (Yellow Spring Instruments).

### Indirect Calorimetry

Metabolic rate was measured by indirect calorimetry in open-circuit Oxymax chambers, a component of the Comprehensive Lab Animal Monitoring System (CLAMS; Columbus Instruments, Columbus, OH). Mice were housed individually and maintained at 23°C under a 12hr light/12hr dark cycle. Food and water were available *ad libitum*.

### Glucose and insulin tolerance tests

For GTTs, mice were fasted overnight. Glucose (2g/kg) was administered intraperitoneally (IP), and blood glucose levels were measured at 0, 15, 30, 60, and 120 min. Serum insulin was measured during the GTT at the 0, 15 and 60 min time points. For the ITT, mice were fasted for 6 hours. Insulin (0.7U/kg for chow diet and 0.8U/kg for HFD) was administered IP, and blood glucose measured at 0, 15, 30, 60, and 120min.

### Determination of cellular respiration

Tissue respiration was performed using a Clark electrode (Strathkelvin Instruments). Freshly isolated BAT was isolated, rinsed in sterile saline, weighed, minced, and placed into respiration buffer, and readings were taken with three separate pieces of tissue of equivalent size. Oxygen consumption was normalized to tissue weight. For Seahorse studies, BAT mitochondria were isolated in STE buffer, pH 7.4 (250mM sucrose, 5mM Tris, 2mM EGTA). Mitochondria were resuspended in assay buffer (50mM KCl, 4mM $KH_2PO4$, 5mM HEPES, and 1mM EGTA, 4% BSA, 10mM Pyruvate, 5mM Malate). Oxygen consumption rate (OCR) of BAT mitochondria (5 μg) was determined using an XF24 Extracellular Flux Analyzer (Seahorse Bioscience). Uncoupled and maximal OCR was determined using oligomycin (14μM) and FCCP (10μM). Antimycin A and rotenone (4μM each) were used to inhibit Complex III- and Complex I- dependent respiration.

### Luciferase reporter assays

The mouse *Ucp1* promoter was amplified and inserted into the KpnI and XhoI sites of pGL3-basic (Promega). HEK293T cells were cultured in 24-well plates and co-transfected with PGC-1α plasmid (0.2ug/well), IRF4 plasmid (0.2ug/well), luciferase reporter construct (0.2ug/well), and galactosidase expression vector (control reporter) (0.006 ug/well) with the Profection™ kit (Promega), according to the manufacturer's protocol. The mass of transfected plasmids was balanced with empty vector (pCDH-EGFP). After 48h, cells were harvested and measured using the Dual-Luciferase Reporter assay system (Promega), and luciferase activity was divided by Renilla luciferase activity (control reporter) to normalize for transfection efficiency. Alternatively, SVFs were extracted from BAT and then six days after adipogenic stimulation, adipocytes were detached with trypsin and transfected using

the Amaxa nucleofection system (Amaxa Biosystems). Transfections were performed with 1μg reporter construct along with 0.5μg IRF4-pCDH expression vector, 1 μg pcDNA-PGC-1α with 25 ng galactosidase expression vector. After 48 h, cells were harvested and measured using the Dual-Luciferase Reporter assay system (Promega). All luciferase assay experiments were performed 3 times at least, and each conducted in triplicate.

### Chromatin Immunoprecipitation (ChIP)

Nuclei were extracted from BAT of BATI4OE mice and then treated with 1% formaldehyde for 4 min at room temperature to cross-link DNA-protein complexes. Genomic DNA was sheared with a Sonic Dismembrator Model 100 (Fisher Scientific) to obtain fragments ranging from 200 bp to 1 kb. ChIP was performed with a kit from Upstate, with 10 μg primary antibody from Santa Cruz (goat anti-IRF4; sc-6059) or goat IgG. Cross-linking was reversed and purified DNA was subjected to QPCR with SYBR green fluorescent dye (Stratagene).

### Protein extraction and Western blot analysis

Protein was extracted from BAT by using RIPA buffer (Boston BioProducts) supplemented with complete protease inhibitor cocktail (Roche). For Western blot analyses, 60 mg protein was subjected to SDS-PAGE under reducing conditions, transferred, and blotted with an appropriate antibody.

### Co-immunoprecipitation studies

HEK293T cells were transfected with IRF4, PGC-1α, or both. Cell lysates were collected in RIPA buffer 48h after transfection. IRF4 protein was immunoprecipitated using anti-IRF4 antibody (sc-28696; Santa Cruz). IRF4 was western blotted using anti-IRF4 antibody (sc-6059; Santa Cruz) and anti-PGC-1α antibody (AB3242; Millipore).

### GST-pull down

GST-PGC-1α vector was a gift from Pere Puigserver, and was transformed into BL21 (NEB) to express the protein. IRF4 was synthesized using a TNT-coupled *in vitro* transcription/translation system (Promega). The resultant protein was incubated with GST-PGC-1α and then immobilized on glutathione-Sepharose beads according to the manufacturer's instructions (Thermo). Proteins were eluted by glutathione and analyzed by western blotting.

### Analysis of gene expression by Q-PCR

Total RNA was extracted from tissues with TRIzol reagent (Invitrogen) according to the manufacturer's instructions. 1ug total RNA was converted into first-strand cDNA with oligo(dT) primers as described by the manufacturer (Clontech). PCR was performed in an Mx3000P Q-PCR system (Stratagene) with specific primers and SYBR Green PCR Master Mix (Stratagene). The relative abundance of mRNAs was standardized with 36B4 mRNA as the invariant control.

### Adenovirus production, purification, and injection

The adenoviral expression vector pAD/CMV/V5-DEST (Invitrogen) encoding cDNA for PGC-1α and Lac Z were constructed as per manufacturer's protocol. Crude adenovirus were amplified twice and then purified using the Vivapure adenopack-100 purification kit (Sartorius Stedim). Adenovirus titer was calculated using Adeno-X Rapid Titer kit (Clontech). For fat pad injections, Lac Z or PGC-1α adenovirus (1×10^10 ifu/mice) were injected subcutaneously into the inguinal fat pad in a total volume of 50ul.

### Statistical Analysis

Unpaired two-tailed Student's t-tests and two-way ANOVA were used. $p<0.05$ was considered statistically significant.

## Supplementary Material

Refer to Web version on PubMed Central for supplementary material.

## Acknowledgments

The authors gratefully acknowledge Ulf Klein (Columbia University) for the *Irf4*$^{flox}$ *mice*. PGC-1α constructs were the gift of Pere Puigserver; other plasmids were from Lisa Madisen and Hongkui Zeng. The Electron Microscopy core of the BIDMC performed the EM analysis. We thank members of the Rosen and Spiegelman laboratories, and Saverio Cinti, for helpful discussions and technical advice. This work was funded by an AHA Post-doctoral Fellowship to XK, NIH R01 DK31405 to BMS, and NIH R01 DK085171 to EDR.

## References

Alon U. Network motifs: theory and experimental approaches. Nature reviews Genetics. 2007; 8:450–461.

Altarejos JY, Montminy M. CREB and the CRTC co-activators: sensors for hormonal and metabolic signals. Nature reviews Molecular cell biology. 2011; 12:141–151.

Boyer BB, Kozak LP. The mitochondrial uncoupling protein gene in brown fat: correlation between DNase I hypersensitivity and expression in transgenic mice. Molecular and cellular biology. 1991; 11:4147–4156. [PubMed: 1712903]

Brustle A, Heink S, Huber M, Rosenplanter C, Stadelmann C, Yu P, Arpaia E, Mak TW, Kamradt T, Lohoff M. The development of inflammatory T(H)-17 cells requires interferon-regulatory factor 4. Nature immunology. 2007; 8:958–966. [PubMed: 17676043]

Cretney E, Xin A, Shi W, Minnich M, Masson F, Miasari M, Belz GT, Smyth GK, Busslinger M, Nutt SL, et al. The transcription factors Blimp-1 and IRF4 jointly control the differentiation and function of effector regulatory T cells. Nature immunology. 2011; 12:304–311. [PubMed: 21378976]

Cypess AM, Lehman S, Williams G, Tal I, Rodman D, Goldfine AB, Kuo FC, Palmer EL, Tseng YH, Doria A, et al. Identification and importance of brown adipose tissue in adult humans. The New England journal of medicine. 2009; 360:1509–1517. [PubMed: 19357406]

Cypess AM, White AP, Vernochet C, Schulz TJ, Xue R, Sass CA, Huang TL, Roberts-Toler C, Weiner LS, Sze C, et al. Anatomical localization, gene expression profiling and functional characterization of adult human neck brown fat. Nature medicine. 2013; 19:635–639.

Eguchi J, Kong X, Tenta M, Wang X, Kang S, Rosen ED. Interferon regulatory factor 4 regulates obesity-induced inflammation through regulation of adipose tissue macrophage polarization. Diabetes. 2013

Eguchi J, Wang X, Yu S, Kershaw EE, Chiu PC, Dushay J, Estall JL, Klein U, Maratos-Flier E, Rosen ED. Transcriptional control of adipose lipid handling by IRF4. Cell metabolism. 2011; 13:249–259. [PubMed: 21356515]

Eguchi J, Yan QW, Schones DE, Kamal M, Hsu CH, Zhang MQ, Crawford GE, Rosen ED. Interferon regulatory factors are transcriptional regulators of adipogenesis. Cell metabolism. 2008; 7:86–94. [PubMed: 18177728]

Ferrer MD, Tauler P, Sureda A, Tur JA, Pons A. Antioxidant regulatory mechanisms in neutrophils and lymphocytes after intense exercise. Journal of sports sciences. 2009; 27:49–58. [PubMed: 19031335]

Giguere V. Transcriptional control of energy homeostasis by the estrogen-related receptors. Endocrine reviews. 2008; 29:677–696. [PubMed: 18664618]

Guerra C, Navarro P, Valverde AM, Arribas M, Bruning J, Kozak LP, Kahn CR, Benito M. Brown adipose tissue-specific insulin receptor knockout shows diabetic phenotype without insulin resistance. The Journal of clinical investigation. 2001; 108:1205–1213. [PubMed: 11602628]

Honda K, Taniguchi T. IRFs: master regulators of signalling by Toll-like receptors and cytosolic pattern-recognition receptors. Nature reviews Immunology. 2006; 6:644–658.

Huss JM, Kopp RP, Kelly DP. Peroxisome proliferator-activated receptor coactivator-1αlpha (PGC-1αlpha) coactivates the cardiac-enriched nuclear receptors estrogen-related receptor-alpha and -gamma. Identification of novel leucine-rich interaction motif within PGC-1alpha. The Journal of biological chemistry. 2002; 277:40265–40274. [PubMed: 12181319]

Jiang DS, Bian ZY, Zhang Y, Zhang SM, Liu Y, Zhang R, Chen Y, Yang Q, Zhang XD, Fan GC, et al. Role of interferon regulatory factor 4 in the regulation of pathological cardiac hypertrophy. Hypertension. 2013; 61:1193–1202. [PubMed: 23589561]

Kajimura S, Seale P, Kubota K, Lunsford E, Frangioni JV, Gygi SP, Spiegelman BM. Initiation of myoblast to brown fat switch by a PRDM16-C/EBP-beta transcriptional complex. Nature. 2009; 460:1154–1158. [PubMed: 19641492]

Kajimura S, Seale P, Spiegelman BM. Transcriptional control of brown fat development. Cell metabolism. 2010; 11:257–262. [PubMed: 20374957]

Kajimura S, Seale P, Tomaru T, Erdjument-Bromage H, Cooper MP, Ruas JL, Chin S, Tempst P, Lazar MA, Spiegelman BM. Regulation of the brown and white fat gene programs through a PRDM16/CtBP transcriptional complex. Genes & development. 2008; 22:1397–1409. [PubMed: 18483224]

Klein U, Casola S, Cattoretti G, Shen Q, Lia M, Mo T, Ludwig T, Rajewsky K, Dalla-Favera R. Transcription factor IRF4 controls plasma cell differentiation and class-switch recombination. Nature immunology. 2006; 7:773–782. [PubMed: 16767092]

Kleiner S, Mepani RJ, Laznik D, Ye L, Jurczak MJ, Jornayvaz FR, Estall JL, Chatterjee Bhowmick D, Shulman GI, Spiegelman BM. Development of insulin resistance in mice lacking PGC-1αlpha in adipose tissues. Proceedings of the National Academy of Sciences of the United States of America. 2012; 109:9635–9640. [PubMed: 22645355]

Kozak UC, Kopecky J, Teisinger J, Enerback S, Boyer B, Kozak LP. An upstream enhancer regulating brown-fat-specific expression of the mitochondrial uncoupling protein gene. Molecular and cellular biology. 1994; 14:59–67. [PubMed: 8264627]

Kwon H, Thierry-Mieg D, Thierry-Mieg J, Kim HP, Oh J, Tunyaplin C, Carotta S, Donovan CE, Goldman ML, Tailor P, et al. Analysis of interleukin-21-induced Prdm1 gene regulation reveals functional cooperation of STAT3 and IRF4 transcription factors. Immunity. 2009; 31:941–952. [PubMed: 20064451]

Larose M, Cassard-Doulcier AM, Fleury C, Serra F, Champigny O, Bouillaud F, Ricquier D. Essential cis-acting elements in rat uncoupling protein gene are in an enhancer containing a complex retinoic acid response domain. The Journal of biological chemistry. 1996; 271:31533–31542. [PubMed: 8940169]

Liew CW, Boucher J, Cheong JK, Vernochet C, Koh HJ, Mallol C, Townsend K, Langin D, Kawamori D, Hu J, et al. Ablation of TRIP-Br2, a regulator of fat lipolysis, thermogenesis and oxidative metabolism, prevents diet-induced obesity and insulin resistance. Nature medicine. 2013; 19:217–226.

Man K, Miasari M, Shi W, Xin A, Henstridge DC, Preston S, Pellegrini M, Belz GT, Smyth GK, Febbraio MA, et al. The transcription factor IRF4 is essential for TCR affinity-mediated metabolic

programming and clonal expansion of T cells. Nature immunology. 2013; 14:1155–1165. [PubMed: 24056747]

Manfredi LH, Zanon NM, Garofalo MA, Navegantes LC, Kettelhut IC. Effect of short-term cold exposure on skeletal muscle protein breakdown in rats. J Appl Physiol (1985). 2013; 115:1496–1505. [PubMed: 23908317]

Meirhaeghe A, Crowley V, Lenaghan C, Lelliott C, Green K, Stewart A, Hart K, Schinner S, Sethi JK, Yeo G, et al. Characterization of the human, mouse and rat PGC1 beta (peroxisome-proliferator-activated receptor-gamma co-activator 1 beta) gene in vitro and in vivo. The Biochemical journal. 2003; 373:155–165. [PubMed: 12678921]

Nguyen KD, Qiu Y, Cui X, Goh YP, Mwangi J, David T, Mukundan L, Brombacher F, Locksley RM, Chawla A. Alternatively activated macrophages produce catecholamines to sustain adaptive thermogenesis. Nature. 2011; 480:104–108. [PubMed: 22101429]

Odegaard JI, Chawla A. The immune system as a sensor of the metabolic state. Immunity. 2013; 38:644–654. [PubMed: 23601683]

Ortega-Molina A, Efeyan A, Lopez-Guadamillas E, Munoz-Martin M, Gomez-Lopez G, Canamero M, Mulero F, Pastor J, Martinez S, Romanos E, et al. Pten positively regulates brown adipose function, energy expenditure, and longevity. Cell metabolism. 2012; 15:382–394. [PubMed: 22405073]

Puigserver P, Spiegelman BM. Peroxisome proliferator-activated receptor-gamma coactivator 1 alpha (PGC-1 alpha): transcriptional coactivator and metabolic regulator. Endocrine reviews. 2003; 24:78–90. [PubMed: 12588810]

Raczkowski F, Ritter J, Heesch K, Schumacher V, Guralnik A, Hocker L, Raifer H, Klein M, Bopp T, Harb H, et al. The transcription factor Interferon Regulatory Factor 4 is required for the generation of protective effector CD8+ T cells. Proceedings of the National Academy of Sciences of the United States of America. 2013; 110:15019–15024. [PubMed: 23980171]

Rajakumari S, Wu J, Ishibashi J, Lim HW, Giang AH, Won KJ, Reed RR, Seale P. EBF2 determines and maintains brown adipocyte identity. Cell metabolism. 2013; 17:562–574. [PubMed: 23499423]

Ricquier D, Bouillaud F, Toumelin P, Mory G, Bazin R, Arch J, Penicaud L. Expression of uncoupling protein mRNA in thermogenic or weakly thermogenic brown adipose tissue. Evidence for a rapid beta-adrenoreceptor-mediated and transcriptionally regulated step during activation of thermogenesis. The Journal of biological chemistry. 1986; 261:13905–13910. [PubMed: 3021720]

Saito M, Okamatsu-Ogura Y, Matsushita M, Watanabe K, Yoneshiro T, Nio-Kobayashi J, Iwanaga T, Miyagawa M, Kameya T, Nakada K, et al. High incidence of metabolically active brown adipose tissue in healthy adult humans: effects of cold exposure and adiposity. Diabetes. 2009; 58:1526–1531. [PubMed: 19401428]

Satoh T, Takeuchi O, Vandenbon A, Yasuda K, Tanaka Y, Kumagai Y, Miyake T, Matsushita K, Okazaki T, Saitoh T, et al. The Jmjd3-Irf4 axis regulates M2 macrophage polarization and host responses against helminth infection. Nature immunology. 2010; 11:936–944. [PubMed: 20729857]

Schreiber SN, Knutti D, Brogli K, Uhlmann T, Kralli A. The transcriptional coactivator PGC-1 regulates the expression and activity of the orphan nuclear receptor estrogen-related receptor alpha (ERRalpha). The Journal of biological chemistry. 2003; 278:9013–9018. [PubMed: 12522104]

Sciammas R, Shaffer AL, Schatz JH, Zhao H, Staudt LM, Singh H. Graded expression of interferon regulatory factor-4 coordinates isotype switching with plasma cell differentiation. Immunity. 2006; 25:225–236. [PubMed: 16919487]

Seale P, Bjork B, Yang W, Kajimura S, Chin S, Kuang S, Scime A, Devarakonda S, Conroe HM, Erdjument-Bromage H, et al. PRDM16 controls a brown fat/skeletal muscle switch. Nature. 2008; 454:961–967. [PubMed: 18719582]

Seale P, Kajimura S, Yang W, Chin S, Rohas LM, Uldry M, Tavernier G, Langin D, Spiegelman BM. Transcriptional control of brown fat determination by PRDM16. Cell metabolism. 2007; 6:38–54. [PubMed: 17618855]

Staudt V, Bothur E, Klein M, Lingnau K, Reuter S, Grebe N, Gerlitzki B, Hoffmann M, Ulges A, Taube C, et al. Interferon-regulatory factor 4 is essential for the developmental program of T helper 9 cells. Immunity. 2010; 33:192–202. [PubMed: 20674401]

Tokuyama K, Himms-Hagen J. Brown adipose tissue thermogenesis, torpor, and obesity of glutamate-treated mice. The American journal of physiology. 1986; 251:E407–415. [PubMed: 2876642]

van Marken Lichtenbelt WD, Vanhommerig JW, Smulders NM, Drossaerts JM, Kemerink GJ, Bouvy ND, Schrauwen P, Teule GJ. Cold-activated brown adipose tissue in healthy men. The New England journal of medicine. 2009; 360:1500–1508. [PubMed: 19357405]

Vijgen GH, Bouvy ND, Teule GJ, Brans B, Schrauwen P, van Marken Lichtenbelt WD. Brown adipose tissue in morbidly obese subjects. PloS one. 2011; 6:e17247. [PubMed: 21390318]

Villarroya F, Vidal-Puig A. Beyond the sympathetic tone: the new brown fat activators. Cell metabolism. 2013; 17:638–643. [PubMed: 23583169]

Villena JA, Hock MB, Chang WY, Barcas JE, Giguere V, Kralli A. Orphan nuclear receptor estrogen-related receptor alpha is essential for adaptive thermogenesis. Proceedings of the National Academy of Sciences of the United States of America. 2007; 104:1418–1423. [PubMed: 17229846]

Virtanen KA, Lidell ME, Orava J, Heglind M, Westergren R, Niemi T, Taittonen M, Laine J, Savisto NJ, Enerback S, et al. Functional brown adipose tissue in healthy adults. The New England journal of medicine. 2009; 360:1518–1525. [PubMed: 19357407]

Wang QA, Tao C, Gupta RK, Scherer PE. Tracking adipogenesis during white adipose tissue development, expansion and regeneration. Nature medicine. 2013

Wu J, Bostrom P, Sparks LM, Ye L, Choi JH, Giang AH, Khandekar M, Virtanen KA, Nuutila P, Schaart G, et al. Beige adipocytes are a distinct type of thermogenic fat cell in mouse and human. Cell. 2012; 150:366–376. [PubMed: 22796012]

Wu J, Cohen P, Spiegelman BM. Adaptive thermogenesis in adipocytes: is beige the new brown? Genes & development. 2013; 27:234–250. [PubMed: 23388824]

Wu Z, Boss O. Targeting PGC-1 alpha to control energy homeostasis. Expert opinion on therapeutic targets. 2007; 11:1329–1338. [PubMed: 17907962]

Wu Z, Puigserver P, Andersson U, Zhang C, Adelmant G, Mootha V, Troy A, Cinti S, Lowell B, Scarpulla RC, et al. Mechanisms controlling mitochondrial biogenesis and respiration through the thermogenic coactivator PGC-1. Cell. 1999; 98:115–124. [PubMed: 10412986]

Xue B, Coulter A, Rim JS, Koza RA, Kozak LP. Transcriptional synergy and the regulation of Ucp1 during brown adipocyte induction in white fat depots. Molecular and cellular biology. 2005; 25:8311–8322. [PubMed: 16135818]

Yao S, Buzo BF, Pham D, Jiang L, Taparowsky EJ, Kaplan MH, Sun J. Interferon Regulatory Factor 4 Sustains CD8 T Cell Expansion and Effector Differentiation. Immunity. 2013

Ye L, Wu J, Cohen P, Kazak L, Khandekar MJ, Jedrychowski MP, Zeng X, Gygi SP, Spiegelman BM. Fat cells directly sense temperature to activate thermogenesis. Proceedings of the National Academy of Sciences of the United States of America. 2013; 110:12480–12485. [PubMed: 23818608]

Zheng Y, Chaudhry A, Kas A, deRoos P, Kim JM, Chu TT, Corcoran L, Treuting P, Klein U, Rudensky AY. Regulatory T-cell suppressor program co-opts transcription factor IRF4 to control T(H)2 responses. Nature. 2009; 458:351–356. [PubMed: 19182775]

## Highlights

- IRF4 is induced by cold and cAMP in mouse and human brown adipocytes
- Targeted overexpression of IRF4 promotes thermogenesis and leanness
- Loss of IRF4 reduces thermogenesis and causes obesity and cold intolerance
- IRF4 interacts physically and functionally with PGC-1α to promote thermogenesis

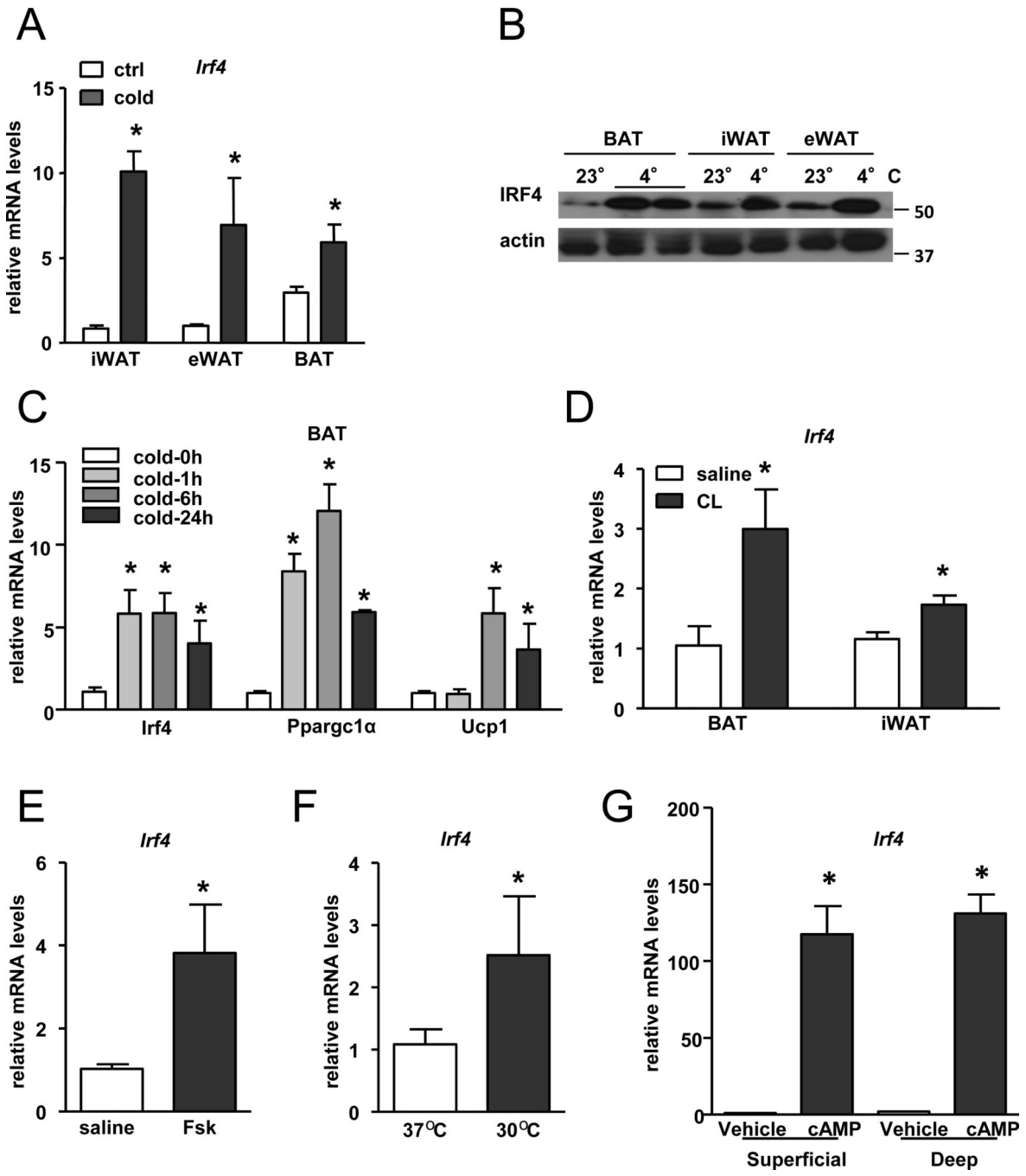


**Figure 1. *Irf4* expression is induced by cold exposure and β3-AR agonist in adipocytes**

***A, B***, QPCR and Western blotting were performed on mRNA and protein from fat depots of C57BL/6 mice at RT or exposed to 4°C for 6 hours. ***C***, QPCR was performed on mRNA from BAT of C57BL/6 mice exposed to 4°C for the indicated lengths of time. N=5. ***D***, Mice were treated with CL316,243 for 6h prior to tissue harvest and QPCR. ***E***, SVF from inguinal fat was differentiated into adipocytes *ex vivo*, treated with Forskolin for 4h, then analyzed by QPCR. ***F***, 3T3-F442A adipocytes were differentiated and cultured at 37°C or 30°C for 10 days followed by harvest and QPCR. ***G***, SVF from superficial and deep neck adipose tissue

depots from four human subjects were differentiated into mature adipocytes and treated for 4h with 500 mM dibutyryl-cAMP. For all parts, *$p < 0.05$, expressed as mean ± SEM.

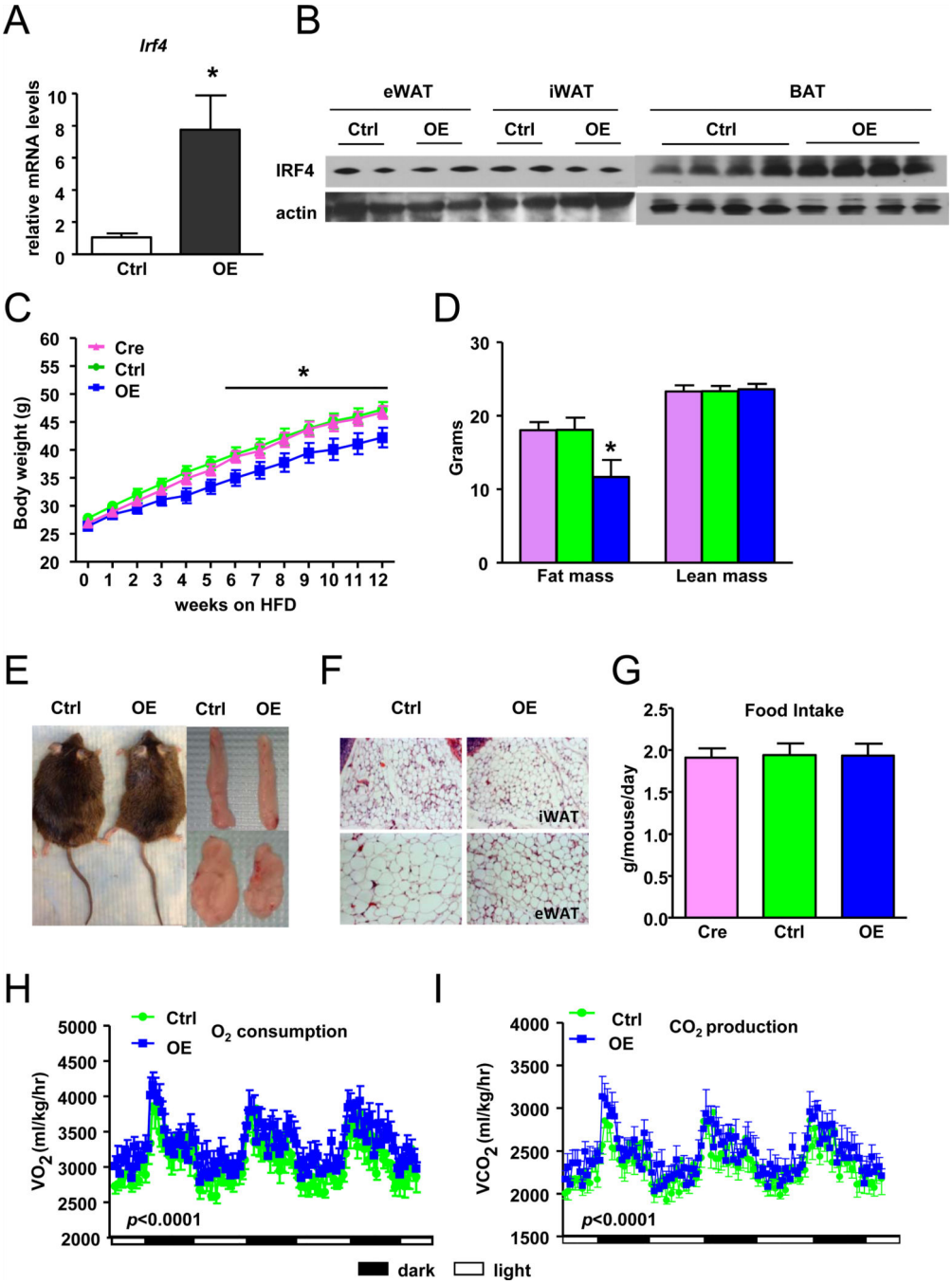


**Figure 2. Mice that overexpress IRF4 in BAT (BATI4OE) are lean and display evidence of enhanced energy expenditure**

***A, B***, IRF4 overexpression was verified in BATI4OE mice by QPCR and Western blotting. Data are normalized to 36B4 and expressed as mean ± SEM (n=4, **p*<0.05). Control mice for all BATI4OE experiments are R26-LSL-IRF4;Cre$^{-}$. ***C***, Body weight of BATI4OE mice on HFD (n=9–16/group, **p*<0.05). ***D***, Body composition of mice from ***C*** after 12 weeks of high-fat feeding (**p*<0.05). ***E***, Gross morphology of BATI4OE mice (36 weeks old) and inguinal and epididymal fat pads after high-fat feeding. ***F***, Hematoxylin and eosin staining

of paraffin-embedded inguinal and epididymal WAT sections from 36-week-old mice (X20). ***G***, Food intake was measured daily after 3 weeks on HFD (n=8), and cumulative food intake was calculated after 3 days. ***H, I***, $O_2$ consumption and $CO_2$ production rates of BATI4OE and WT littermates were measured by indirect calorimetry using CLAMS after 4 weeks on HFD (n=8; **p*<0.0001 for both). See also Supplemental Figures S1 and S2.

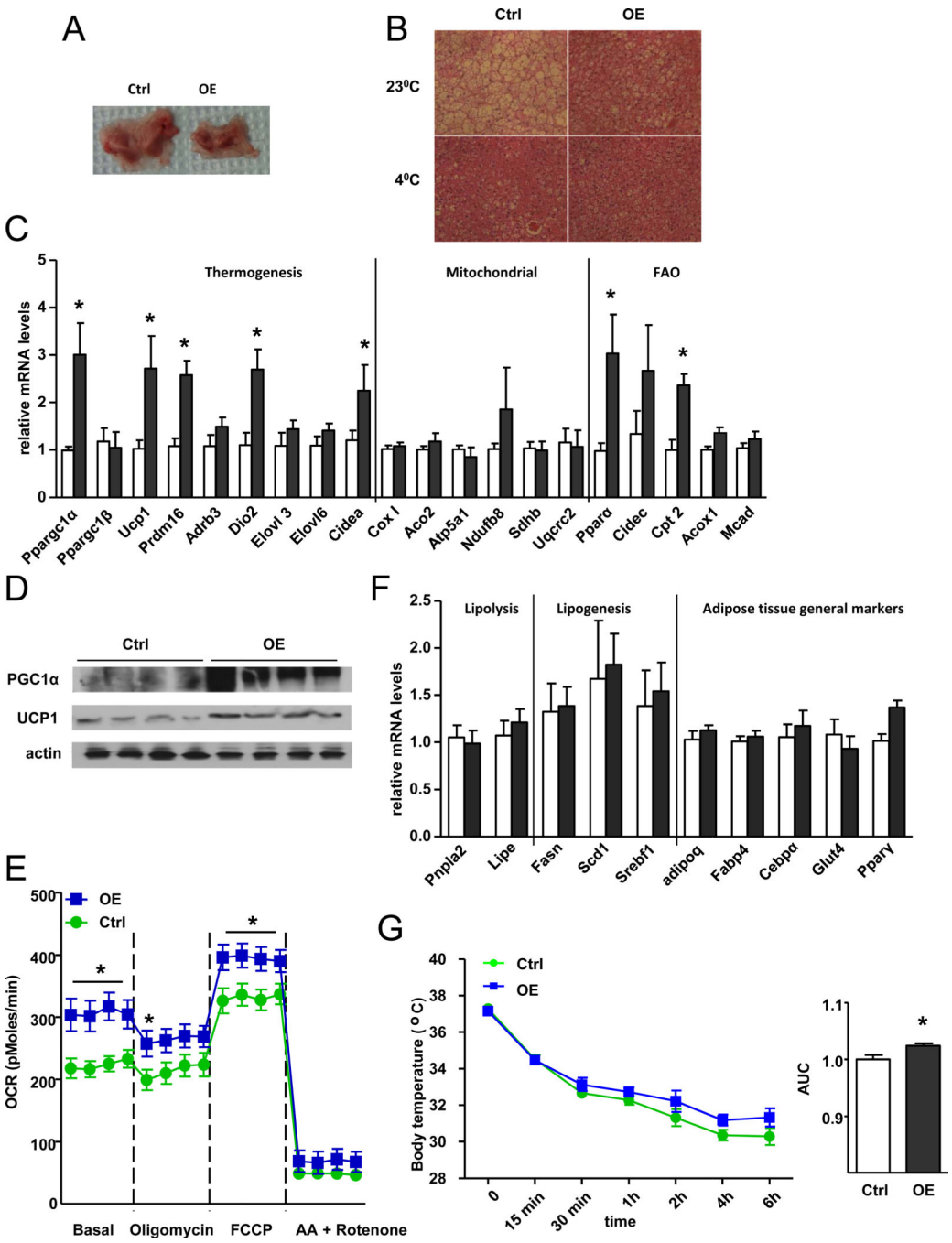


**Figure 3. BATI4OE mice display increased thermogenic gene expression and cold tolerance**

***A***, Gross appearance of interscapular BAT from control and BATI4OE mice at RT. ***B***, Hematoxylin and eosin staining of BAT sections from control and BATI4OE mice housed at 23°C or 4°C for 6hrs. ***C***, Thermogenic, mitochondrial and fatty acid oxidation gene expression in BAT. RNA was harvested from BAT of BATI4OE and control littermates after 28 weeks on HFD at 23°C. Gene expression was measured using QPCR. Data are normalized to *36B4* and expressed as mean ± SEM (n=3–5, **p*<0.05). ***D***, Western blot analysis of protein in BAT of mice from ***C. E***, Continuous measurement of oxygen

consumption rate (OCR) in isolated mitochondria from BAT of BATI4OE and control mice on chow. Oxygen consumption was performed under basal conditions, following the addition of oligomycin (14μM), the pharmacological uncoupler FCCP (10μM) or the Complex III and I inhibitor antimycin A and rotenone (4μM each) (n=10–12, *$p$<0.05). ***F***, Lipid handling and general adipose marker gene expression in BAT. RNA was harvested from BAT of BATI4OE and control littermates after 28 weeks on HFD at 23°C. Gene expression was measured using QPCR. Data are normalized to *36B4* and expressed as mean ±SEM (n=3–5, *$p$<0.05). ***G***, Rectal temperature of control and BATI4OE mice during acute cold exposure (4°C). Results are expressed as mean±SEM (n=6 mice per group, *$p$<0.05 for AUC). See also Supplemental Figure S3.

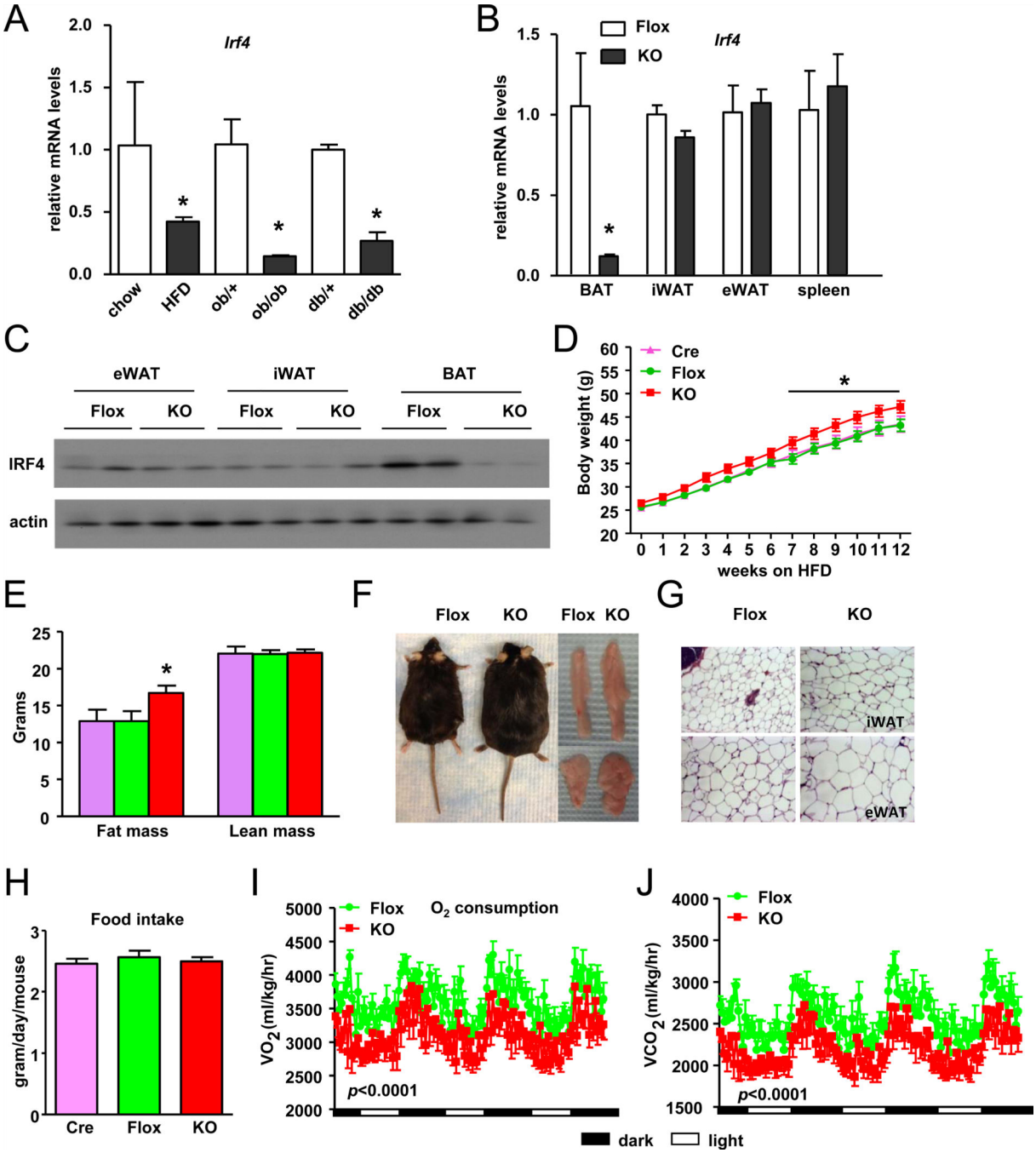


**Figure 4. Mice lacking IRF4 in brown adipose tissue (BATI4KO) have reduced energy expenditure**

***A***, *Irf4* mRNA expression was measured by QPCR in BAT from high-fat diet (HFD), *ob/ob*, and *db/db* mice (n=3–5; **p*<0.05). ***B***, *Irf4* expression in different tissues of BATI4KO and control mice (n=4; **p*<0.05). ***C***, Western blot analysis of IRF4 protein levels in various adipose depots from mice in ***B***. ***D***, Body weights of male Cre only, Flox only and BATI4KO (KO) mice on HFD (n=8–19). ***E***, Body composition of the mice from **C** (**p*<0.05). ***F***, Gross morphology of BATI4KO mice (30 weeks old) and inguinal and epididymal fat pads. ***G***,

Hematoxylin and eosin staining of inguinal and epididymal WAT sections from 30-week-old mice (X20). ***H***, Food intake was measured daily after 20 weeks on HFD (n=8), and cumulative food intake was calculated after 3 days. ***I, J***, $O_2$ consumption and $CO_2$ production rates of BATI4KO and control littermates were measured by indirect calorimetry using CLAMS after 22 weeks on HFD (n=8; **p*<0.0001 for both). See also Supplemental Figure S4.

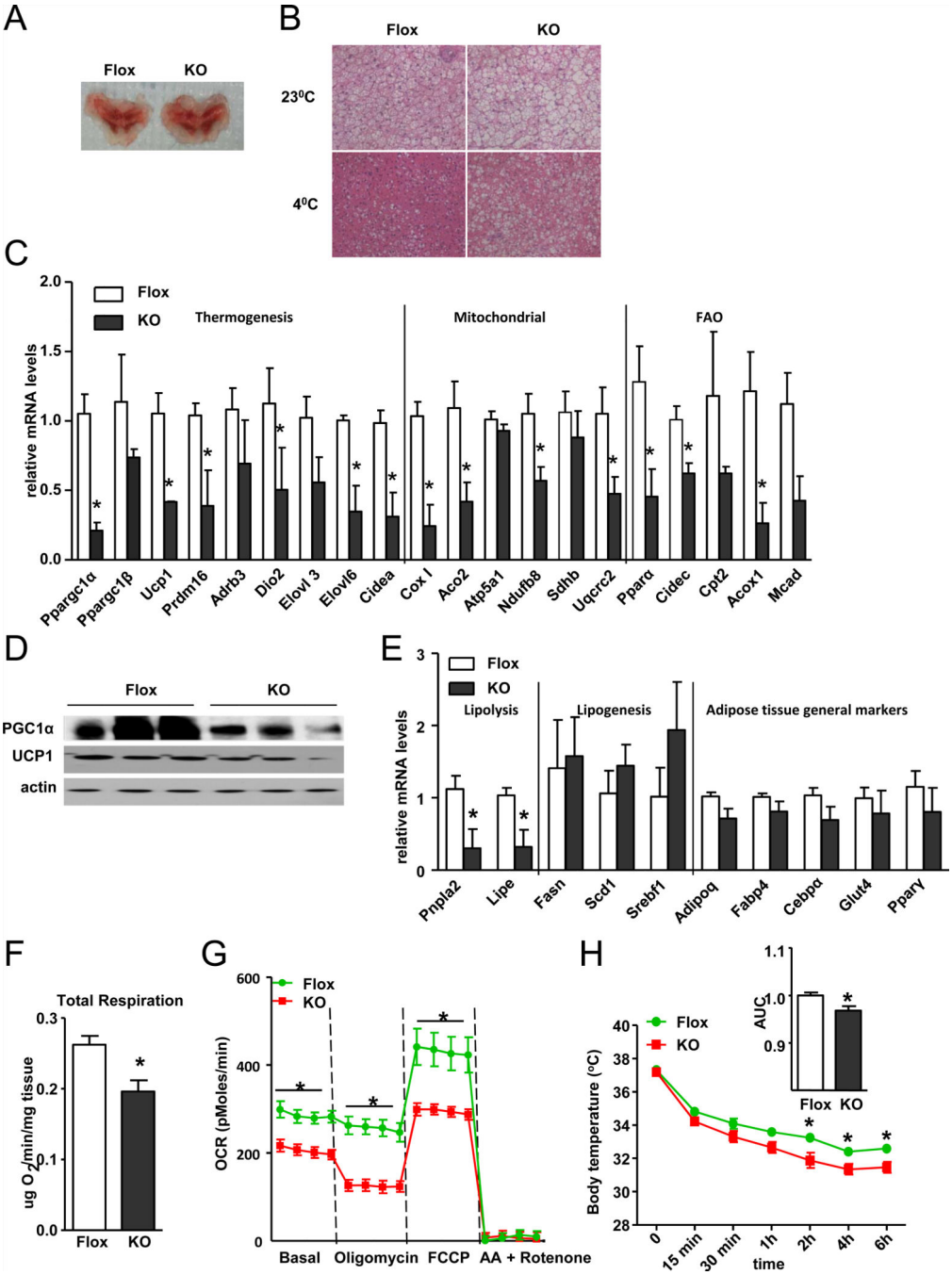


**Figure 5. BATI4KO mice display decreased thermogenic gene expression and cold intolerance**

***A***, Gross appearance of interscapular BAT from control and BATI4OE mice at RT. ***B***, Hematoxylin and eosin staining of BAT sections from mice housed at 23°C or 4°C for 6 hours. ***C***, Thermogenic, mitochondrial and fatty acid oxidation gene expression in BAT. RNA was harvested from BAT of BATI4KO or control littermates after 22 weeks on HFD. Gene expression was measured using QPCR. Data are normalized to *36B4* and expressed as mean ± SEM (n=3–5, **p*<0.05). ***D***, Western blot analysis of protein in BAT of mice in ***C. E***, Lipid handling and general adipose marker gene expression in BAT. RNA was harvested

from BAT of BATI4KO or control littermates after 22 weeks on HFD. Gene expression was measured using QPCR. Data are normalized to *36B4* and expressed as mean ± SEM (n=3–5, **p*<0.05). ***F***, Total respiration in BAT measured by Clark electrode (n=4, **p*<0.05). ***G***, Continuous measurement of oxygen consumption rate (OCR) in isolated mitochondria from BAT of BATI4KO and control mice on chow. Oxygen consumption was performed under basal conditions, following the addition of oligomycin (14μM), the pharmacological uncoupler FCCP (10μM) or the Complex III and I inhibitor antimycin A and rotenone (4μM each) (n=7–13, **p*<0.05). ***H***, Rectal temperature of control and BATI4KO mice during cold exposure (4°C). Results are expressed as mean ± SEM, **p*<0.05 relative to Flox mice (n=6 mice per group). See also Supplemental Figures S5 and S6.

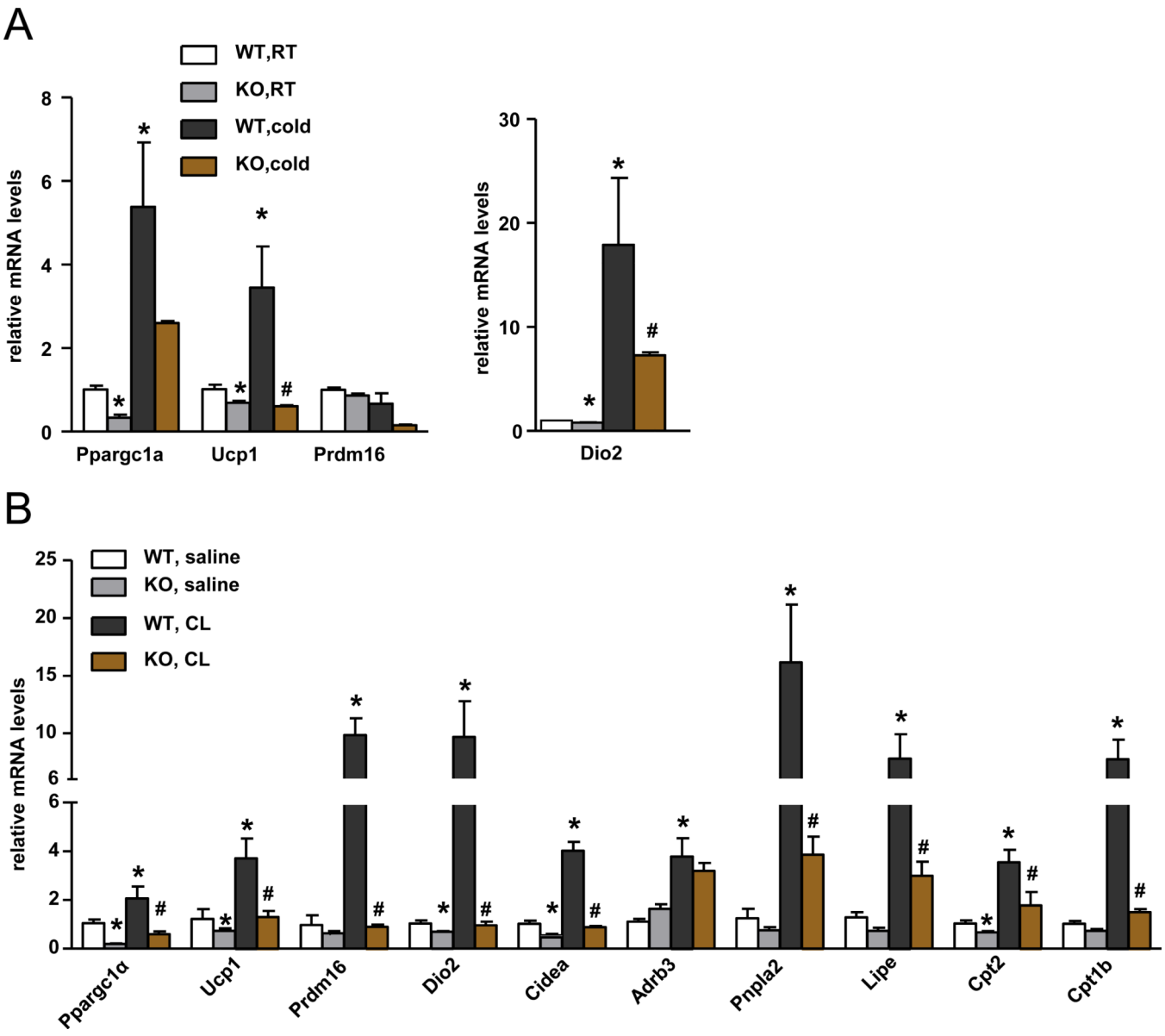


**Figure 6. Cold and β3-agonist cannot induce thermogenic expression in the absence of IRF4**

***A***, RNA was harvested from interscapular BAT of BATI4KO or control littermates housed at 23°C or 4°C for 6hrs. Gene expression was measured using QPCR. Data are normalized to *36B4* and expressed as mean ± SEM (n=3–5, *, *vs* WT RT, $p<0.05$; #, *vs* WT cold, $p<0.05$). ***B***, Mice were treated with CL316,423 or saline for 6hrs and BAT was harvested. Gene expression was analyzed by QPCR. Data are normalized to *36B4* and expressed as mean±SEM (n=3–5, *, *vs* WT saline, $p<0.05$; #, *vs* WT CL, $p<0.05$).

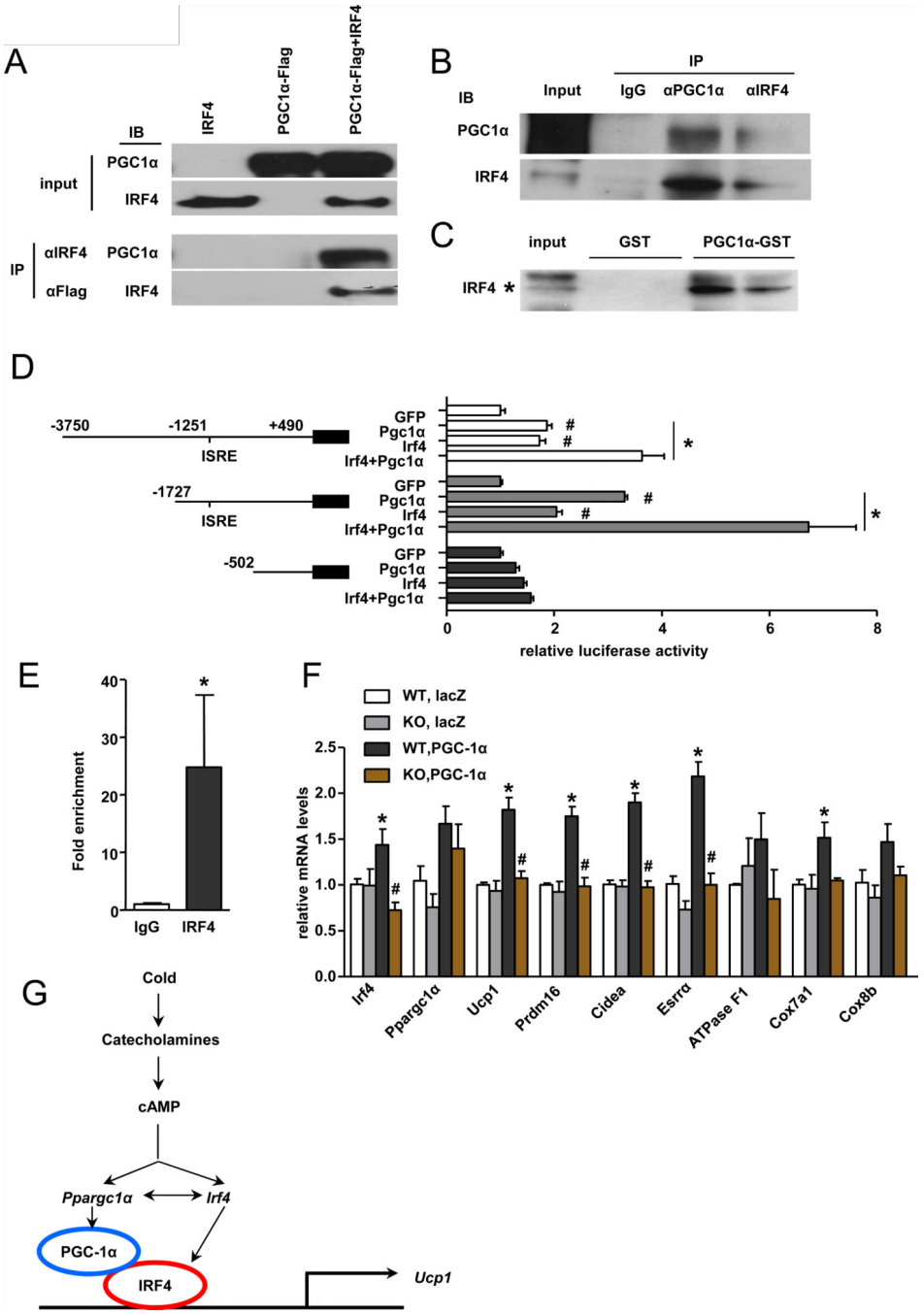


**Figure 7. PGC-1α interacts with IRF4 and enhances its transcriptional activity**

***A***, Co-immunoprecipitation of PGC-1α-FLAG and IRF4 expressed in 293 cells. ***B***, Co-immunoprecipitation of endogenous PGC-1α and IRF4 in BAT of WT mice. Mice were exposed to 4°C for 6hrs and then sacrificed for BAT protein extraction; data represent pooled BAT from 5 animals. ***C***, Direct interaction between PGC-1α and IRF4 by GST-pull down assay. ***D***, Fragments of the *Ucp1* promoter fused to a luciferase reporter gene were cotransfected into 293 cells together with pCDH-GFP (control) or IRF4 in the presence or absence of a PGC-1α expression plasmid. Luciferase activity was corrected for Renilla

luciferase activity and normalized to control activity (n=3, *p<0.05). ***E***, ChIP analysis in BAT from BATI4OE mice. The signal in IgG is set as 1. Results are expressed as mean ± SD (n=3, *$p$<0.05). ***F***, Adenovirus expressing PGC-1α or lacZ was injected into the inguinal fat pad of control or BATI4KO mice (n=3–6, *$p$<0.05). ***G***, Model of how PGC-1α and IRF4 interact at the genetic, physical, and functional levels to promote thermogenic gene expression. See also Supplemental Figure S7.